# Generalized first-principle model of magnetic levitation⋆

František Dušek[a], Jiří Tuček[a], Aleš Novotný[a] and Daniel Honc[a,*]

[a]Faculty of Electrical Engineering and Informatics, University of Pardubice, náměstí Čs. legií 565, Pardubice, 530 02, Czech Republic

ARTICLE INFO

*Keywords*:
magnetic levitation, solenoid inductance, solenoid magnetic force, nonlinear math model

ABSTRACT

Since its first demonstration more than a half century ago, magnetic levitation (MagLev) has gained eminent scientific attention from both the fundamental and applied points of view. In essence, MagLev shows highly nonlinear dynamics, described with nonlinear differential equations. Thus, in order to exploit the MagLev phenomenon, both mathematical models and control algorithms must be constructed. Frequently authors use simplifications of the model, and in doing so, limit the application of the MagLev model around a nominal operating point. In these simplified cases, the MagLev models may contain parameters that are not represented by proper physical quantities. Thus, in this work, we revised the issue of MagLev modelling from the first-principle approach. More specifically, we theoretically derived expressions for the interaction between the magnetic fields of the solenoid and a small magnetic object. The behavior of the inductance on a distance from the solenoid was then described. The suggested MagLev modelling concept was verified experimentally, confirming the validity and correctness of the proposed MagLev mathematical model. The results presented here could thus be regarded as highly beneficial for formulating more complex MagLev designs exploitable in the field of model predictive control of the position of a levitating object.

## 1. Introduction

Magnetic levitation (MagLev), or sometimes referred to as a magnetic suspension, is a physical state when an object floats in a medium with a magnetic field compensating the effect of the gravity and/or other acceleration-causing forces [1, 2]. The MagLev phenomenon emerges when two essential conditions are met: (i) the presence of the lifting magnetic forces acting against the gravitational force in a precisely opposite direction and equal magnitude and (ii) the existence of energetically-favorable stability which encourages a stable and firm configuration of a levitating object in a space. These conditions prevent sliding or dropping from the magnetic-field-induced floating region [1, 2]. The MagLev concept dates back to the 1960s when a friction-free suspension was, for the first time, demonstrated for a graphite disk levitating in a vacuum [3]. Since then, a huge effort has been devoted to theoretically describe and experimentally design and optimize MagLev systems for applications in various fields, from both the microscopic and macroscopic perspective.

The devices based on the MagLev phenomenon use magnets, which are suitably arranged in a space to generate a proper magnetic field with lifting action forces. In general, all types of magnets can be exploited including permanent magnets, electromagnets, ferromagnets, diamagnets, superconductors, and magnetic fields originating from induced electric currents in the conductors [2]. However, considering the Earnshaw's theorem [4], it can be shown that it is not possible for a static system consisting of only paramagnetic and ferromagnetic materials to float in the gravitational field in a stable configuration. This is due to repulsion magnetic forces generally promoting instability, where one of the two magnets always tends to slip away or physically reverse. Thus, in order to reach stability, several strategies have been proposed involving applications of servo-mechanisms [5], diamagnetic materials [6], superconductors [2, 7] or eddy currents [8, 9]. More specifically, materials with a solely diamagnetic response (for which the relative permeability is less than 1) are of eminent interest as they show a static stability along at least one axis (e.g., z-axis). Thus, in the case of the diamagnetic levitation, the equilibrium condition reads as $B\frac{\mathrm{d}B}{\mathrm{d}z} = \frac{\mu_0 \rho g}{\chi}$ [10] where $\mu_0$ is the permeability of the vacuum, $\rho$ represents the density of the diamagnetic material, $g$ denotes the gravitational acceleration, $\chi$ stands for the material's magnetic susceptibility, $B$ is the induction of the magnetic field generated by a magnet at a given point of the space, and $\frac{\mathrm{d}B}{\mathrm{d}z}$ stands for the rate of change of the magnetic field along the z-axis. As superconductors completely expel the external magnetic fields if their values lie well below the characteristic superconductor's critical field, they are regarded as perfect diamagnetic materials (for which $\chi$=-1) and thus ideal candidates in the MagLev systems [2]. Especially, type-II superconductors (i.e., low-temperature superconductors – LTSs) have been found appealing due to their inherent property of flux pinning, further stabilizing the levitation [2]. Recently, high-temperature superconductors (HTSs) based on bismuth strontium calcium copper oxide (BSCCO) and rare-earth barium copper oxide (ReBCO) have been applied. These materials provide higher magnetic fields and sufficiently high operating temperatures [11] and [12]. However, the MagLev technology using both LTSs and HTSs suffers several problems. Temperatures below the liquid nitrogen temperature ($77K$) are required for HTSs to enter and preserve the superconducting state, thus causing high demands for cooling mechanisms. In the case of HTSs and their coils, the technological challenges include suppression of the screening current-induced magnetic field, degradation in the coil performance as a result of extensive

⋆Corresponding authors:
daniel.honc@upce.cz (D. Honc)
ORCID(s):

mechanical stresses, and construction of protective systems minimizing the consequences of the abrupt thermal runaway [11].

Nowadays, the portfolio of MagLev applications is very broad and diverse, covering areas of both fundamental and applied research. Due to elimination of wear and maintenance problems, traditional MagLev examples include frictionless rotors [13], magnetic bearings [14, 15], flywheels [16, 17], pressure gauges [3], and accelerometers [18]. In the field of transportation, MagLev technology have been heavily exploited for construction of high-speed levitating trains (especially in Japan, China, and Germany) [19, 20], design of high-grade transport devices in clean rooms (in semiconductor or bioengineering industry) [21], or development of spaceship propulsion systems [22]. As a part of miniaturization efforts, MagLev principles have been found effective for micro-manipulation [8] and micro-positioning [23, 24] of the 3D objects in space. Moreover, MagLev plays an eminent role in density-based chemical analysis [25–27], separation processes [28], and contact-less manipulation and trapping of organic diamagnetic substances [29–31]. In the field of analytical chemistry, biochemistry, and biotechnology [32, 33], MagLev technology has been recently proposed for competitive protein-ligand binding assays [34, 35], tissue engineering [36], cell manipulation and culturing [37–39], and biochemical diagnosis [40]. In materials science, MagLev strategies have been identified as promising for crystal growth [10], self-assembly [41, 42], separation of crystal polymorphs in their mixture [43], and defect analysis [44], to name a few. Very recently, MagLev architectures have been designed and used for electromagnetic energy harvesting, providing low-cost and customizable electric power [45–49].

In terms of orientation of magnetic forces in the MagLev configurations, those of either repulsive or attractive nature can be employed [50, 51]. In the case of the repulsive MagLev alternative, sometimes referred to as an electrodynamic suspension, levitation forces are generated by superconductors or permanent magnets. Electrodynamic suspension is partially stable, providing a large clearance. On the other hand, the attractive MagLev case, also known as an electromagnetic suspension, suffers from an inherent instability resulting in difficult control with feedback systems. In a general perspective, it is necessary to control all the six axes of motion in space, i.e., three translational and three rotational degrees of freedom [52]. In essence, MagLev shows highly nonlinear dynamics, described with nonlinear differential equations [53]. Moreover, a significant open-loop instability often occurs, further complicating the formulation of the MagLev mathematical model. Thus, several parameters must be monitored in real time to maintain stability conditions. These include measurements of the position and velocity of the levitated object, electric currents in the electromagnetic coils, parasitic resistance and inductance due to coil heating, etc. These parameters are required as input variables for construction of the high-performance feedback controller. To do so, two different approaches are generally followed [54–63]. In most cases, a linearized MagLev model is constructed; however, it is applicable only around a nominal operating point and does not consider any eventual variations of the parameters. If nonlinearities appear, they are frequently accounted for in the mathematical models with the help of $\mu$-synthesis, backstepping, gain scheduling, proportional–integral-derivative (PID) controllers with notch filters, fuzzy neural network-based controllers, and/or fractional order controllers [62, 64–67]. The other possibility is to directly solve the MagLev nonlinear differential equations at a given point and time. So far, the effort has been limited only to simulations, as real-time solving is computationally very demanding.

Motivated by the immense significance of MagLev technology, we address the issue of description and modelling of the MagLev technique from the first-principle perspective. More specifically, in the present study, we focused on finding the relation expressing the mutual interaction between the magnetic fields from a solenoid and a passive object. Magnetization of the object is generated only by the applied magnetic field. As a result, a force equation is derived, describing the effect of the magnetic field along the solenoid axis on a small object (i.e., a ball) of ferromagnetic nature. In addition, the introduced approach yields a relationship for a dependence of the inductance on a distance from the solenoid. In order to experimentally validate the derived equations, a laboratory device (i.e., "Magnetic Levitation CE152" module) was employed. We constructed a simplified nonlinear dynamic model when all its parameters have physical meaning and are represented by proper physical quantities. The values of the inductance parameters based on the distance from the solenoid were evaluated from the measured courses of the control voltage of the current amplifier of the solenoid and the voltage of the ball position sensor. Based on the comparison of the values of the calculated parameters with those expected, and the error of the model depending on the distance of the object from the coil, we then discussed the validity and correctness of the relations for describing the magnetic field strength of the solenoid acting on the small ball object.

## 2. The magnetic field of a coil

The force of the magnetic field acting on an object depends on the magnetic field intensity and the object properties. In this work, it is considered that the object is a sphere made of a ferromagnetic material with a diameter $d$ and able to move only in the axis of solenoid with a radius $r_c$ and a length $l_c$. Furthermore, derived relationships are based on the assumption that $l_c \gg 2r_c \gg d$.

### 2.1. The intensity of the magnetic field

The magnetic field intensity at the point on the axis of the closed current loop with a constant current $i$ is described by the Biot-Savart-Laplace law (1), i.e.,

$$\mathrm{d}H = i\frac{\mathrm{d}l \times p^0}{4\pi p^2}. \tag{1}$$

Figure 1 shows a contribution $dH$ to the overall intensity $H$ of the magnetic field at a point in a distance $y$ on the axis of the current loop with a radius $r$ which is invoked by an element of a length $dl$. Due to the symmetry, the resulting intensity is the sum of all the elements contributions, i.e.,

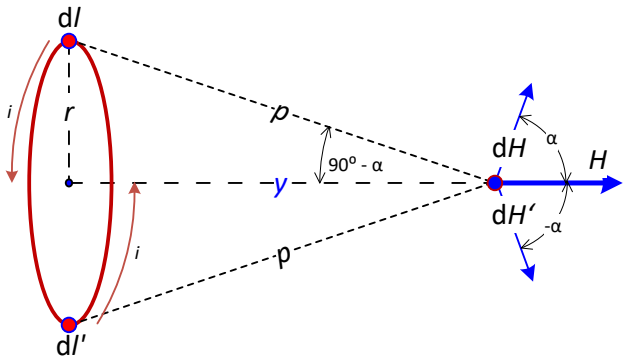


**Figure 1:** The intensity in the circle loop axis.

$$H = \oint \cos(\alpha)\mathrm{d}H = \oint \frac{i\cos(\alpha)}{4\pi p^2}|\mathrm{d}l \times p^0|. \tag{2}$$

Because the intensity $\mathrm{d}H$ is constant for all the elements, and is perpendicular to the vector $p$, then $|\mathrm{d}l \times p^0| = \mathrm{d}l$. The angle $\alpha$ is constant during the integration; thus, Eg. (2) can be written as

$$H = \frac{i\cos(\alpha)}{4\pi p^2}\oint \mathrm{d}l = \frac{i\cos(\alpha)}{4\pi p^2}2\pi r = \frac{r}{2p^2}\cos(\alpha)\, i. \tag{3}$$

Considering relations that $p^2 = r^2 + y^2$ and $\cos(\alpha) = \frac{r}{p}$, deduced from the geometric arrangement of the problem, it is possible to derive Eg. (4), describing the intensity of the magnetic field at a point in a distance $y$ on the axis of the current loop, i.e.,

$$H = \frac{r^2}{2p^3}i = \frac{r^2}{2\left(r^2 + y^2\right)^{\frac{3}{2}}}\, i. \tag{4}$$

In the case of a cylinder (see Figure 2) with a length $L$ and a radius $r$, it is assumed that the magnetic field is induced by a surface current flowing on the surface of the cylinder. If the total surface current is $j$, then a surface current $\mathrm{d}j = j\mathrm{d}\epsilon$ flows through the ring with a width $\mathrm{d}\epsilon$. Then the contribution $\mathrm{d}H$ of this surface current to the total intensity $H$ in the solenoid axis and distance $y$ is

$$\mathrm{d}H = \frac{r^2 j}{2\left(r^2 + y^2\right)^{\frac{3}{2}}}\mathrm{d}\epsilon \tag{5}$$

and the total intensity $H$ is

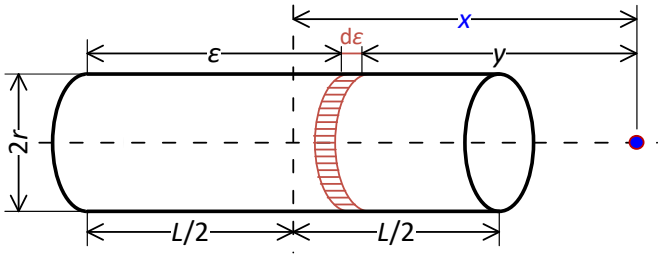


**Figure 2:** The intensity in the solenoid axis.

$$H = \int_{\epsilon=0}^{L}\mathrm{d}H = \int_{\epsilon=0}^{L}\frac{r^2 j}{2\left(r^2 + y^2\right)^{\frac{3}{2}}}\mathrm{d}\epsilon. \tag{6}$$

After substituting $y = \frac{L}{2} + x - \epsilon$ and $\mathrm{d}y = -\mathrm{d}\epsilon$ and evaluating the integral, the equation, describing the solenoid magnetic field intensity in the solenoid axis and distance $x$ from the solenoid centre, is given as

$$H = \frac{r^2}{2}j\int_{x+\frac{L}{2}}^{x-\frac{L}{2}}\frac{-\mathrm{d}y}{\left(r^2 + y^2\right)^{\frac{3}{2}}} = \frac{j}{2}f_{L,r}(x)\ [A.m^{-1}], \tag{7a}$$

$$f_{\mathrm{L,r}}(x) = \left[\frac{x + \frac{L}{2}}{\sqrt{\left(x + \frac{L}{2}\right)^2 + r^2}} - \frac{x - \frac{L}{2}}{\sqrt{\left(x - \frac{L}{2}\right)^2 + r^2}}\right] \quad |x| \geq \frac{L}{2}. \tag{7b}$$

## 2.2. The magnetic field intensity of a coil with a core

If a solenoid with $Z$ loops and constant current $i$ is considered instead of the cylinder, the magnetic field intensity $H$ in the solenoid axis can be expressed, depending on the coil geometry and the distance $x$ from the centre of the solenoid, as

$$H(x) = \frac{1}{2}\frac{Zi}{L}f_{\mathrm{L,r}}(x). \tag{8}$$

If a solenoid with the core is considered, assuming that the core is made of a magnetically soft material with magnetization $M$, Eq. (8) can be rewritten to

$$H(x) = \frac{1}{2}\left(\frac{Zi}{L} + M\right)f_{\mathrm{L,r}}(x). \tag{9}$$

Now, let us assume that the magnetization/demagnetization of the coil core $M$ do not show any hysteresis, and up to the saturation magnetization $M_{\max}$, it linearly depends on the magnetic field intensity $H$ inside the coil. In this case, we can write that

$$i \geq i_{\max} \rightarrow M = M_{\max}, \tag{10a}$$

$$0 < i < i_{\max} \rightarrow M = \frac{M_{\max}}{i_{\max}} i. \tag{10b}$$

Finally, under the above mentioned assumptions and restrictions, the magnetic field intensity $H$ in the coil axis can be expressed as

$$H(x) = \frac{1}{2}\left(\frac{Z}{L} + \frac{M_{\max}}{i_{\max}}\right) i f_{\mathrm{L,r}}(x), \qquad 0 < i < i_{\max}, \tag{11}$$

Here, $f_{\mathrm{L,r}}(x)$ describes a dependence of the magnetic field intensity inside the solenoid on a distance $x$ from the coil centre, with a radius $r$ and a length $L$.

### 2.3. The magnetic force acting on the ball

Furthermore, it is considered that the object is a ball with a diameter $d$ made of a ferromagnetic material with a relative permeability $\mu_{\mathrm{r}} \gg 1$. The assumptions for determining magnetization $M_k$ are as follows:

1. a magnetization/demagnetization does not show any hysteresis (a magnetically soft feature);
2. a magnetization $M$ is up to the saturation induced by the surrounding magnetic field intensity $H$;
3. the ball is sufficiently small; thus, it is possible to assume that the magnetization $M$ distribution is constant in the whole ball volume and solely depends on the magnetic field intensity $H$ in the ball centre.

For example, let us start from the mathematical expression for a space magnetization with known susceptibility. The magnetization $M$ of a linear magnet with a magnetic susceptibility $\chi_m$, exposed to an external magnetic field of an intensity $H$, can be written as

$$M = \chi_m H. \tag{12}$$

The intensity $H_k$ of the magnetic field inside the ball made of the material with the magnetic susceptibility $\chi_m$, located in the external magnetic field with the intensity $H$, is then

$$H_k = \frac{1}{1 + \frac{\chi_m}{3}} H. \tag{13}$$

The magnetic susceptibility $\chi_m$ can be replaced by the relative permeability $\mu_r$, i.e.,

$$\mu_{\mathrm{r}} = 1 + \chi_m = \mu_k. \tag{14}$$

Thus, it is possible to express the dependence of the ball magnetization $M_k$ with the relative permeability $\mu_k$ on the intensity $H$ of the surrounding magnetic field [68, (8.86)], i.e.,

$$M_k = \frac{\chi_m}{1 + \frac{\chi_m}{3}} H = \frac{3(\mu_k - 1)}{2 + \mu_k} H. \tag{15}$$

If it is assumed that the movement of the object occurs only in the axis of a solenoid, then the field intensity changes only in one axis. The force $F(x)$, which arises due to the magnetic field with the intensity $H$ acting on an object with volume $V$ and magnetization $M$, can be expressed considering the relation for the magnetic energy accumulated within this object [68, (10.24a)], [69, (36.24)], i.e.,

$$E = \frac{1}{2}\mu_0 H \int_V M \mathrm{d}V = \frac{1}{2}\mu_0 V_k \frac{3(\mu_k - 1)}{2 + \mu_k} H^2(x), \tag{16a}$$

$$F(x) = \frac{\partial E}{\partial x} = k_k i^2 f_{L,r}(x) \frac{\mathrm{d} f_{\mathrm{L,r}}(x)}{\mathrm{d}x} \tag{16b}$$

where $\mu_0$ $[H \cdot m^{-1} = kg \cdot m \cdot s^{-2} \cdot A^{-2}]$ is the permeability of vacuum, $\mu_k$ stands for the relative permeability of an object material, and $k_k = \frac{4}{3}\pi \left(\frac{d}{2}\right)^3 \frac{3(\mu_k - 1)}{2 + \mu_k} \mu_0 \left[\frac{1}{2}\left(\frac{Z}{L} + \frac{M_{max}}{i_{max}}\right)\right]^2$.

### 2.4. The inductance in the coil axis as a distance function

As shown later when constructing the MagLev mathematical model, it is preferable to consider the inductance $L$ instead of the magnetic field intensity $H$. If the force of the magnetic field acting on an object is known, i.e., given by Eq. (16b), it is possible to express the inductance $L$ from the definition of the magnetic field energy [70, (12.5)], i.e., $E = \frac{1}{2}Li^2$ $F(i,x) = \frac{\partial}{\partial x}E(i,x) = i^2 \frac{\mathrm{d}}{\mathrm{d}x}L(x)$, as

$$L(x) = \int \frac{F(i,x)}{i^2} \mathrm{d}x = L_1 + L_0 f^2_{\mathrm{L,r}}(x), \tag{17}$$

where $L_1 = L_\infty = \mu \frac{Z^2}{L} S$ $S = \pi r^2$ is the inductance of a solenoid (coil) with a cross-sectional area $S$. Here, it is assumed that $L \gg r$ [68, (8.39)].

## 3. Mathematical model of the magnetic levitation device

The mathematical model (i.e., a system of the differential and algebraic equations) describes the simplified ideal behaviour of a real MagLev device - laboratory Magnetic Levitation System (MLS) (see Figure 3) [71]. The model features the dependence of a voltage $y(t)$ of the sensor measuring ball distance (from the bottom) on the control input voltage $u(t)$ of the current amplifier. The ball distance from the coil $x(t)$ is one of the model state variables.

### 3.1. The device description and the default relationships

The basic device scheme with marked variables and geometric parameters is shown in Figure 4. The current $i(t)$


**Figure 3:** Laboratory plant CE152.

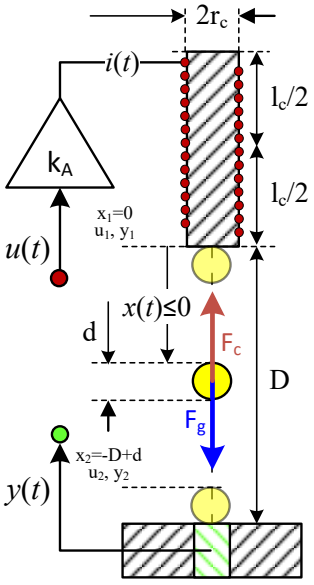


**Figure 4:** The device scheme.

flows through the coil, which has a radius $r_c$ and a length $l_c$, and is generated by a current amplifier with a gain $k_A$ controlled by the input control voltage $u(t)$. It is assumed that a small ball with a mass $m$ and a diameter $d$ is moving only in the coil axis inside the area between the coil front and a pad (distance $D$). Furthermore, it is considered that the ball and the coil core are made of a magnetically soft material, whose magnetization/demagnetization behaves linearly without any hysteresis. The ball position $x(t)$ – measured from the coil front, i.e., $-(D-d) < x < 0$ – is measured by the induction position sensor located in the pad, which converts the ball distance from the sensor to the voltage

**Table 1**
The calibration of the position sensor.

| Sensor voltage | Ball position | Parameters | |
|---|---|---|---|
| $y$ [V] | $x$ [m] | $a$ [V.m$^{-1}$] | $b$ [V] |
| 4.830 | 0 | 842.4561 | 4.830 |
| 0.028 | $-(d-D)$ =-0.0057 | | |

$y(t)$ linearly. The device can be divided into three separate subsystems.

### 3.1.1. *The position sensor subsystem*

The position sensor subsystem is described by a dependence of the output voltage of the sensor on the ball position $x(t)$. According to the manufacturer details, this relationship is linear inside a part of the measured distance range, i.e.,

$$y(t) = ax(t) + b \qquad [V], \tag{18a}$$

$$x_{\min} < |x| < x_{\max} \qquad [m]. \tag{18b}$$

The parameters $a, b$ are determined by a separate experiment when a sensor voltage $y_1$ was measured at a ball position $x_1 = 0$ (the ball near the coil) and a voltage $y_2$ at a ball position $x_2$ (the ball near the sensor). The position $x_2$ is selected as a negative distance of the coil bottom from the sensor minus the ball diameter. The parameters from Eq. (18) – $a = 842.4561$, $b = 4.830$ – are determined from the measurement in the limit positions as shown in Table 1.

### 3.1.2. *The current amplifier and coil subsystem*

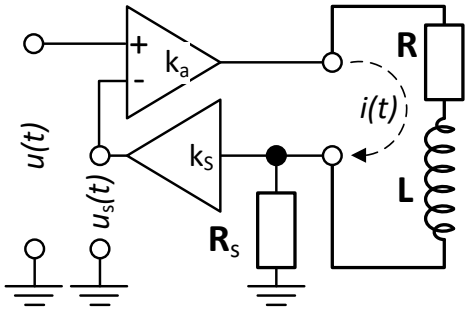


**Figure 5:** The current amplifier scheme.

The second subsystem is formed by a coil with a current amplifier. Equation (19) is based on the energy balance of the coil and describes a dependence between voltage $u(t)$ and the current $i(t)$ which flows through the coil with a winding resistance $R$. Thus,

$$u = \frac{\mathrm{d}\phi}{\mathrm{d}t} + Ri(t) \qquad [V], \tag{19}$$

where $\phi$ is the magnetic flow, i.e., $\phi = L(x)i(t)$, and $L(x)$ represents the inductance of the coil in the coil axis, dependent on the distance $x(t)$ from its centre.

**Table 2**
Nominal values of current amplifier.

| Symbol | Value | Units | Description |
|---|---|---|---|
| $k_a$ | 100 | [-] | Amp. gain |
| $k_s$ | 13.33 | [-] | Close loop gain |
| $R_s$ | 0.25 | [Ω] | Close loop resistance |
| $R$ | 3.5 | [Ω] | Coil resistance |
| $L$ | 0.03 | [H] | Static coil inductance (also $L_\infty$) |
| $k_A = \frac{k_a}{R_L}$ | 0.297 | [$\Omega^{-1}$] | |

Equation (19) needs to be modified to include a current amplifier used for the device. The coil current amplifier block diagram is shown in Figure 5 with the relevant parameters listed (and determined by nominal values) in Table 2.

The dependence between the control voltage $u$ and the current $i$ flowing through the coil is then expressed as

$$k_a(u - u_s) = (R + R_s)i + \frac{\mathrm{d}\phi(x,i)}{\mathrm{d}t}, \tag{20a}$$

$$u_s = k_s R_s i. \tag{20b}$$

The coil with the current amplifier can be then mathematically described as

$$k_a u = \frac{\mathrm{d}\phi(x,i)}{\mathrm{d}t} + R_L i(t), \tag{21a}$$

$$R_L = R + R_s(1 + k_a k_s), \tag{21b}$$

with a DC (static) gain $i = k_A u$ and $k_A = \frac{k_a}{R_L} = 0.297$.

#### *3.1.3. The ball and coil subsystem*

The third subsystem consists of a ball in the Earth's gravity and the magnetic field of the coil. In the equilibrium state, forces acting on the ball must be balanced as expressed by the general vector equation in the form of

$$\vec{F}_s + \vec{F}_g + \vec{F}_m + \vec{F}_x = 0, \tag{22}$$

where $\vec{F}_s$ is the inertial force, $\vec{F}_g$ represents the weight force, $\vec{F}_m$ stands for the magnetic field force and $\vec{F}_x$ denotes the drag force. The magnitude of forces, features in Eq. (22), are given as

$$F_s(x) = m\frac{\mathrm{d}^2 x}{\mathrm{d}t^2}, \tag{23a}$$

$$F_g = mg, \tag{23b}$$

$$F_m(i,x) = \frac{\partial E(i,x)}{\partial x} = \frac{\partial \phi(i,x) i}{\partial x}, \tag{23c}$$

$$F_x(x) = k_x \left(\frac{\mathrm{d}x}{\mathrm{d}t}\right)^2, \tag{23d}$$

where $m$ is ball mass, $g$ represents the free-fall acceleration, $E$ denotes the energy of the coil magnetic field, and $k_x$ stands for the drag coefficient.

When considering the orientation of the forces according to Figure 4 and their dependence on the inductance $L(x)$, Eq. (22) can be modified to a set of Eqs. (24), which describe the ideal behaviour of the studied MagLev device, i.e.,

$$m\frac{\mathrm{d}^2 x}{\mathrm{d}t} + k_x \frac{\mathrm{d}x}{\mathrm{d}t}\left|\frac{\mathrm{d}x}{\mathrm{d}t}\right| = \frac{1}{2}\frac{\partial L(x)}{\partial x} i^2 - mg, \tag{24a}$$

$$\frac{\partial L(x)}{\partial x}\frac{\mathrm{d}x}{\mathrm{d}t} i + L(x)\frac{\mathrm{d}i}{\mathrm{d}t} = k_a u(t) - R_L i, \tag{24b}$$

$$y(t) = ax + b. \tag{24c}$$

### 3.2. Mathematical model of the MagLev device

Finally, the function $f_{\mathrm{L,r}}(x)$ from Eq. (7b) is modified to express the dependence on a position $x \leq 0$, measured from the from lower bound of the coil (see Figure 2), i.e., $x = x_c - \frac{l_c}{2}$, where $x_c$ is distance measured from the coil centre. Thus

$$f(x) = \frac{x}{\sqrt{x^2 + r_c^2}} - \frac{x - l_c}{\sqrt{(x - l_c)^2 + r_c^2}} \text{ for } x \leq 0. \tag{25}$$

An ideal non-linear dynamic mathematical device model, expressed by a set of Eqs. (26), describes the dependence of the output sensor voltage $y(t)$ on the control input voltage $u(t)$ of the coil. The dimensionless function $f(x)$ is given by Eq. (25). The model is based on a set of Eqs. (24), where the dependence of inductance, given by Eq. (17), on the position $x \leq 0$ from the coil bottom edge is involved. Then

$$\frac{\mathrm{d}x}{\mathrm{d}t} = v, \tag{26a}$$

$$\frac{\mathrm{d}v}{\mathrm{d}t} = \frac{L_0}{m} f(x)\frac{\partial f(x)}{\partial x} i^2 - g - \frac{k_x}{m} v|v|, \tag{26b}$$

$$[L_1 + L_0 f^2(x)]\frac{\mathrm{d}i}{\mathrm{d}t} = k_a u - (R_L + 2L_0 f(x)\frac{\partial f(x)}{\partial x} v) i, \tag{26c}$$

$$y = ax + b, \tag{26d}$$

where $v$ [$m \cdot s^{-1}$] is the velocity of the ball in the coil axis.

## 4. Experiments and results

Experiments on the real MagLev device were carried out to verify the validity of the derived Eq. (16b) of the force acting on an object depending on the distance from the coil. If the current $i$ and the distance from the coil $x$ are known at particular stable ball positions, then it is possible to calculate the values of a static model parameters, given by a set of Eqs. (27), thus fulfilling a criterion that the calculated magnetic force approaches the gravity force as much as possible (i.e., a balance condition). Since all the parameters are of physical importance, it is possible to deduce the credibility of the model from the calculated values of the parameters and from the force differences.

### 4.1. Static model

In the case when the ball is stabilized in a constant position (levitation), the magnetic force is equal to the weight and the dynamic model, given by a set of Eqs. (26), is transformed into the static model, expressed by a set of Eqs. (27) (here, the position and the current is constant). The values of the parameters are listed in Table 3. Hence,

$$g = \frac{L_0}{m} f(x_n) \left.\frac{\partial f(x)}{\partial x}\right|_{x=x_n} i_n^2, \tag{27a}$$

$$y_n = a x_n + b, \tag{27b}$$

$$i_n = k_a u_n, \tag{27c}$$

The steady-states positions were measured both in the gradual closing of the ball to the coil and during delaying. Thus, the magnetization of the coil core and the ball increased when the ball was closing and decreased when the ball was delaying. This arrangement allowed to determine whether magnetization/demagnetization is accompanied with the hysteresis phenomena.

### 4.2. Determination of the static model parameters

The parameters $L_0$, $l_c$, and $r_c$ of the static model, given by a set of Eqs. (27), were determined from the control and measured voltages in 24 steady-states (balanced) measured positions in the range of 10 % and 90 % of a distance between the sensor and the coil bottom edge.

#### *4.2.1. The steady-states measurements*

A measurement of the sensor voltage and the control voltage generation were performed using the MF634 acquisition card [72] in the MATLAB environment. The used computer allowed to use a 1 ms sampling. Since the steady-state positions are unstable, it was necessary to maintain them by the feedback control. To achieve and maintain the specified sensor voltage, a discrete PSD controller with a filtration of the desired value for a smoother change transition of the desired voltage was used. To compensate the controlled system non-linearity, the system was supplemented by the calculation of the steady-state control voltage to the required voltage. For this calculation, a simplified non-linear static model, described by Eq. (28a), originating from the simpler inductance dependence on a distance, given by Eq. (28b), was adopted. The parameters $L_0$, $x_0$ of the simplified model were determined from the two measured steady states (the ball near the coil and the ball near the sensor). Thus

**Table 3**
Determination of the static model values.

| Symbol | Value | Units | Description |
|---|---|---|---|
| $g$ | 9.81 | $[m \cdot s^{-2}]$ | free-fall acceleration |
| $m$ | 0.00828 | $[kg]$ | mass of the ball |
| $k_A$ | 0.287 | $[A \cdot V^{-1}]$ | gain of the current amplifier (21) |
| $a$ | 842.4561 | $[V \cdot m^{-1}]$ | conv. par. position to voltage (18) |
| $b$ | 4.830 | $[V]$ | conv. par. position to voltage (18) |
| $L_1$ | 0.03 | $[H]$ | static coil inductance |
| $L_0$ | 0.0 | $[H]$ | dynamic coil ind. (optimized par.) |
| $l_c$ | 0.100 | $[m]$ | coil length (optimized parameter) |
| $r_c$ | 0.025 | $[m]$ | coil radius (optimized parameter) |
| $u_n$ | meas. | $[V]$ | control volt. in n-th steady state |
| $y_n$ | meas. | $[V]$ | output volt. in n-th steady state |
| $i_n$ | calc. | $[A]$ | coil current in n-th steady state |
| $x_n$ | calc. | $[m]$ | ball position in n-th steady state |

$$g = \frac{1}{2mx_0} \frac{L_0}{\left(1 + \frac{x}{x_0}\right)^2} k_A^2 u^2, \tag{28a}$$

$$L(x) = L_1 + \frac{L_0}{1 + \frac{x}{x_0}}. \tag{28b}$$

The actual measurement for 12 voltage values evenly distributed between 10 % and 90 % of the possible range of the ball position was provided by an automatic experiment. After stabilizing to the lowest voltage level (the ball being closest to the sensor), 2 seconds were left to switch to a higher level until the highest level (the ball being closest to the coil) was reached, and then the levels gradually decreased. In this way, 12 measurements were obtained when magnetizations of the coil core and the ball were increasing, and another 12 measurements when the magnetizations were decreasing.

24 sensor voltage values $y(x)$ and the corresponding control voltage values $u(x)$ were acquired from the regulation of the ball position (see Figure 6). The values of both voltages were evaluated as the arithmetic average of 1000 measured values from a 1-sec interval before the next change. The measurement was repeated 4-times with 10 minutes delays between each experiment to verify repeatability and ensure that the temperature of the coil would not affect the experiment.

#### *4.2.2. The evaluation of the measured steady-states positions*

The standard deviation (STD) error of the difference between the acceleration caused by the magnetic field and

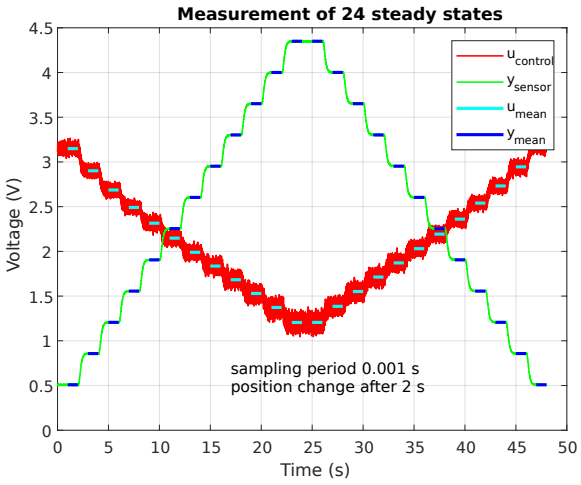


**Figure 6:** Measurement and evaluation of steady states - experiment 4

free-fall acceleration was minimized from the 24 steady-states voltages by a choice of 3 parameters, given in a set of Eq. (29). The accelerations were used for evaluation instead of the forces because acceleration differences give a better illustration of the physical meaning of the difference.

$$\mathrm{STD} = \sqrt{\frac{1}{23}\sum_{j=1}^{24}\left(g - \frac{1}{2m}i_j^2\frac{\partial}{\partial x}L(x_j;\boldsymbol{p})\right)^2}, \tag{29a}$$

$$\boldsymbol{p}_{opt} = \arg\min_{\boldsymbol{p}} \mathrm{STD}(\boldsymbol{p}), \tag{29b}$$

$$i_j = k_A u_j, \tag{29c}$$

$$x_j = \frac{y_j - b}{a}, \tag{29d}$$

$$L(x;\boldsymbol{p}) = L_1 + L_0 f^2(x), \tag{29e}$$

$$\boldsymbol{p} = \begin{bmatrix} L_0 \\ l_c \\ r_c \end{bmatrix}. \tag{29f}$$

Values of the parameters obtained by an minimization in a set of Eqs. (29) for each dataset are summarized in Table 4.

## 5. Discussion

In Section 2, we derived Eq. (16b) for the force acting in a solenoid axis on a small sphere made of a ferromagnetic soft material. From this equation, we then derived Eq. (17) for the inductance of a coil with a core as a function of the distance from the coil. These expressions were applied in Section 3 for a construction of the particular mathematical model of the studied real MagLev device. In Section 4, we described the measurements of steady states. The measured values were used for determining the parameters of a function describing force (inductance) dependence on the distance from the coil.

**Table 4**
Identified parameters and the model error.

| Measurement | $L_0$ [H] | $l_c$ [mm] | $r_c$ [mm] | STD [m.s$^{-2}$] |
|---|---|---|---|---|
| MerStat00 | 3.300e-03 | 79.21 | 5.973 | 0.949 |
| MerStat01 | 3.315e-03 | 65.16 | 5.966 | 0.948 |
| MerStat02 | 3.327e-03 | 48.05 | 5.977 | 0.952 |
| MerStat03 | 3.319e-03 | 54.50 | 5.969 | 0.957 |

From Table 4, it is evident that the calculated values of the coil dynamic inductance $L_0$ and radius $r_c$ do not dramatically depend on the used dataset. More significant fluctuations occurred in the coil length $l_c$. However, none of the parameters showed unexpected values. The calculated parameters depend on the convention of the ball distance from the coil. The values of the parameters $a$, $b$ are used for a position sensor voltage conversion to distance.

If we study the dependence of the parameter values and standard deviation of a relative error on the experiment order (the effect of the increase of the coil winding temperature caused by experiments by approximately 10 °$C$), then it seems that the temperature change up to 10 °$C$ does not significantly affect the device behaviour.

In Figure 7, we show the calculated values of inductances and the ball accelerations caused by the magnetic field of the coil in steady states. The static model with identified parameters was used. For each experiment, and for the changing distance from the coil, the inductance dependence on the position is in the upper graph and the relative deviation of the calculated acceleration from the gravitational acceleration is in the lower graph.

The graphs confirm that although inductance changes and optimization has ensured zero mean value, the progress of the relative deviation exhibits a systematic error. Ideally, the course of the deviation should be zero, i.e., in each steady-state position, the calculated acceleration induced by the magnetic field of the coil should be equal to the gravitational acceleration. If the disagreement was caused only by random effects such as measurement uncertainty, etc., deviations would also have a random character. The measurement uncertainties are suppressed by a significant number of measured samples in a given steady-state position.

From a relative error in opposite directions of movement, it is clear that the model does not include hysteresis of the magnetization of the coil core and the ball. However, if the deviation was caused only by neglecting of hysteresis, then

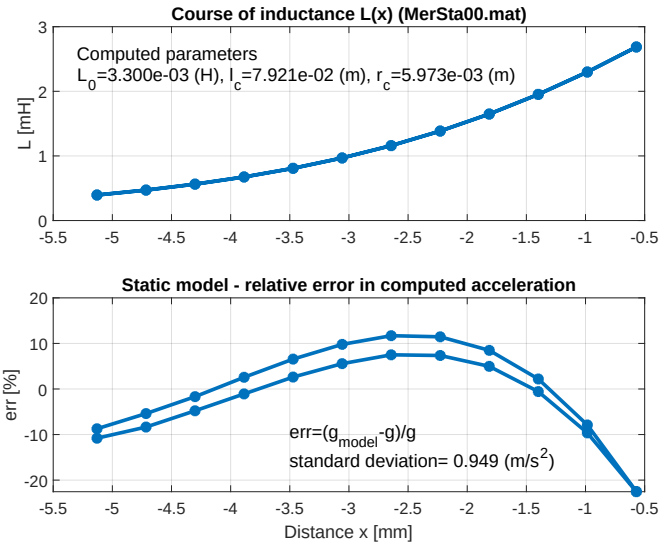


(a) Change in inductance and relative error - experiment 1

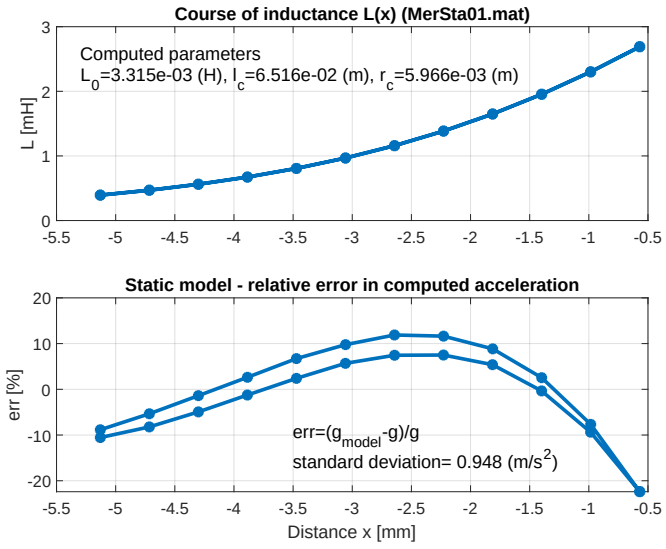


(b) Change in inductance and relative error - experiment 2

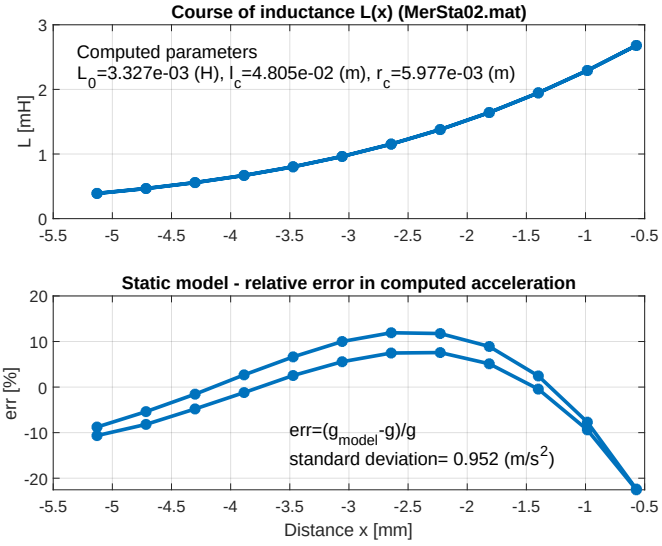


(c) Change in inductance and relative error - experiment 3

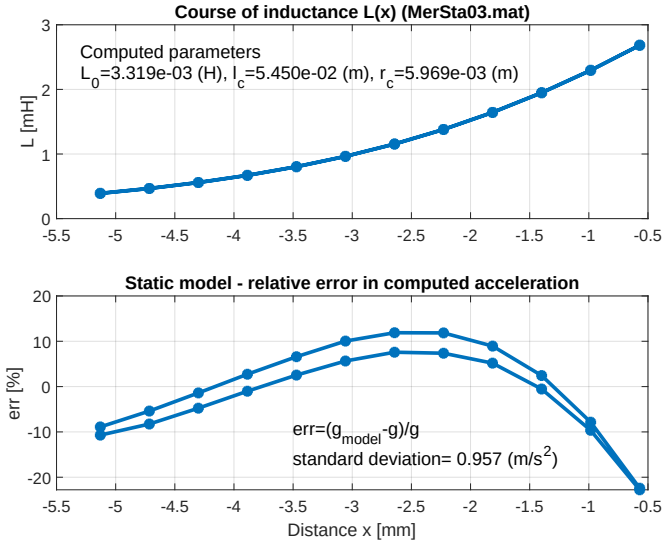


(d) Change in inductance and relative error - experiment 4

**Figure 7:** Error of static model part.

the deviation process would be symmetrical with respect to the $x$-axis during the magnetization and demagnetization.

Obviously, the model approximates the behaviour of the monitored device with a relatively large error. However, it is not possible to clearly decide that the error is caused only by simplification during deriving the equations for the force acting on the object with the ball shape in the magnetic field of the solenoid. Due to the indirect measurement of the position of the ball and the coil current, the deviation can be caused by non-linearity of the position sensor or the current amplifier gain's temperature dependence.

The disadvantage of the device which is used to verify the dependence of the magnetic force on the distance, given by Eq. (16b), is the relatively small range of the ball position. It is likely that the non-linearity caused by small change in a position is not significant due to others factors. Thus, by changing the parameter of the distance function, i.e. Eq. (25), it is not feasible to compensate the model error induced by not included non-linearities.

## 6. Conclusions

In the present work, we studied the MagLev phenomenon from the first-principle perspective. In order to do so, an interaction between the magnetic field from a solenoid and a magnetic response from a ferromagnetic object was considered. Within this MagLev geometry, relations describing both the magnetic force acting on a small ferromagnetic ball, and the spatial behavior of the inductance were derived. More importantly, the proposed force equation was experimentally found to be valid in the entire range of the considered distances. This is in contrast to the commonly adopted relation assuming the magnetic force is inversely proportional to the square of the distance. The force and inductance equations were then used in a construction of

the MagLev mathematical model. Such a sophisticated approach provided solution to the MagLev problem within the framework of the optimal model-based control design.

The presented MagLev concept is regarded beneficial for a construction of more complex mathematical models exploitable in the field of predictive control of the position of a levitating object. In general, if we adopt the model predictive control strategy, it is possible to optimize the subsequent control actions which minimize the chosen criterion on a given time horizon. Within this approach, a dynamical model of the controlled system is needed not only for the calculation of the control action, but also for the state estimation. Thus, the control effects are significantly influenced by the quality of the model. This is crucial especially in cases when we need a fast fulfilment of our requirements (i.e., for tight control). Here, it should be stressed that the system type must be considered when assessing the model quality. For certain systems, the model quality is not so critical - e.g. for single-input single-output (SISO), linear, lower order dynamic systems. On the contrary, model quality will play an eminent role for multi-input multi-output (MIMO), non-linear, higher order dynamic systems, and systems with time delays. Nevertheless, if these conditions and application prerequisites are met, we believe that the modelling methodology, presented here would offer reliable and precise MagLev models for simulations, predictions, and control.

## Disclosure statement

The authors declare no conflict of interest and no competing financial interest.

## Funding

This research was funded by SGS grant of University of Pardubice, Faculty of Electrical Engineering and Informatics.

## CRediT authorship contribution statement

**František Dušek:** Conceptualization, Methodology, Software, Validation, Writing - Original Draft, Visualization, Supervision. **Jiří Tuček:** Validation, Writing - Original Draft, Writing - Review & Editing. **Aleš Novotný:** Software, Validation, Investigation, Writing - Review & Editing. **Daniel Honc:** Conceptualization, Methodology, Validation, Writing - Review & Editing, Supervision, Funding acquisition.

## References

[1] E. H. Brandt, "Levitation in physics," *Science*, vol. 243, no. 4889, pp. 349–355, 1989.

[2] K. Ma, Y. Postrekhin, and W.-K. Chu, "Superconductor and magnet levitation devices," *Review of Scientific Instruments*, vol. 74, pp. 4989–5017, 12 2003.

[3] R. Evrard and G.-A. Boutry, "An absolute micromanometer using diamagnetic levitation," *Journal of Vacuum Science and Technology*, vol. 6, no. 2, pp. 279–288, 1969.

[4] S. Earnshaw, "On the Nature of the Molecular Forces which Regulate the Constitution of the Luminiferous Ether," *Transactions of the Cambridge Philosophical Society*, vol. 7, pp. 98–112, 1842.

[5] D. Ahn, J.-W. Jin, H. Yun, and J. Jeong, "Development of a novel dual servo magnetic levitation stage," in *Actuators*, vol. 11, p. 147, 2022.

[6] Q. Gao, H. Yan, H. Zou, W. Li, Z. Peng, G. Meng, and W. Zhang, "Magnetic levitation using diamagnetism: Mechanism, applications and prospects," *Science China Technological Sciences*, vol. 64, no. 1, pp. 44–58, 2021.

[7] A. Sanchez, N. Del Valle, E. Pardo, D.-X. Chen, and C. Navau, "Magnetic levitation of superconducting bars," *Journal of applied physics*, vol. 99, no. 1, p. 113904, 2006.

[8] C. Elbuken, M. Khamesee, and M. Yavuz, "Eddy current damping for magnetic levitation: Downscaling from macro to micro-levitation," *Journal of Physics D: Applied Physics*, vol. 39, pp. 3932–3938, 2006.

[9] M. Bonvalot, P. Courtois, P. Gillon, and R. Tournier, "Magnetic levitation stabilized by eddy currents," *Journal of magnetism and magnetic materials*, vol. 151, no. 1-2, pp. 283–289, 1995.

[10] M. Motokawa, M. Hamai, T. Sato, I. Mogi, S. Awaji, K. Watanabe, N. Kitamura, and M. Makihara, "Crystal growth and materials processing in the magnetic levitation condition," *Journal of magnetism and magnetic materials*, vol. 226-230, pp. 2090–2093, 2001.

[11] H. Maeda and Y. Yanagisawa, "Recent developments in high-temperature superconducting magnet technology (review)," *IEEE Transactions on applied superconductivity*, vol. 24, no. 3, p. 4602412, 2014.

[12] A. A. Kordyuk, "Magnetic levitation for hard superconductors," *Journal of Applied Physics*, vol. 83, no. 1, pp. 610–612, 1998.

[13] R. D. Waldron, "Diamagnetic levitation using pyrolytic graphite," *Review of Scientific Instruments*, vol. 37, no. 1, p. 29, 1966.

[14] S. Mukhopadhyay, J. Donaldson, G. Sengupta, S. Yamada, C. Chakraborty, and D. Kacprzak, "Fabrication of a repulsive-type magnetic bearing using a novel arrangement of permanent magnets for vertical-rotor suspension," *Magnetics, IEEE Transactions on*, vol. 39, no. 5, pp. 3220 – 3222, 2003.

[15] F. Werfel, U. Floegel-Delor, R. Rothfeld, T. Riedel, B. Goebel, D. Wippich, and P. Schirrmeister, "Superconductor bearings, flywheels and transportation," *Superconductor Science and Technology*, vol. 25, no. 1, p. 014007, 2012.

[16] K. Nagashima, T. Otani, and M. Murakami, "Magnetic interaction between permanent magnets and bulk superconductors," *Physica C: Superconductivity*, vol. 328, no. 3-4, pp. 137–144, 1999.

[17] G. Sotelo, A. Ferreira, and R. de Andrade, "Halbach array superconducting magnetic bearing for a flywheel energy storage system," *IEEE Transactions on Applied Superconductivity*, vol. 15, no. 2, pp. 2253–2256, 2005.

[18] B. Andò, S. Baglio, V. Marletta, A. Valastro, A. Pistorio, and C. Trigona, "A friction less accelerometer exploiting a magnetic levitating mechanism and an inductive readout strategy," in *2017 IEEE International Instrumentation and Measurement Technology Conference (I2MTC)*, pp. 1–5, 2017.

[19] H.-W. Lee, K.-C. Kim, and J. Lee, "Review of maglev train technologies," *IEEE transactions on magnetics*, vol. 42, no. 7, pp. 1917–1925, 2006.

[20] N. Del-Valle, A. Sanchez, C. Navau, and D.-X. Chen, "Magnet guideways for superconducting maglevs: comparison between halbach-type and conventional arrangements of permanent magnets," *Journal of Low Temperature Physics*, vol. 162, no. 1-2, pp. 62–71, 2011.

[21] O. Tsukamoto, K. Yasuda, and J. Chen, "A new magnetic levitation system with ac magnets," *IEEE Transactions on Magnetics*, vol. 24, no. 2, pp. 1497–1500, 1988.

[22] W. Yang, M. Qiu, Y. Liu, Z. Wen, Y. Duan, and X. Chen, "Levitation characteristics in an hts maglev launch assist test vehicle," *Superconductor Science and Technology*, vol. 20, no. 3, pp. 281–286, 2007.

[23] S. Verma, W. jong Kim, and J. Gu, "Six-axis nanopositioning device with precision magnetic levitation technology," *IEEE/ASME Transactions on Mechatronics*, vol. 9, no. 2, pp. 384–391, 2004.

[24] W. jong Kim and D. L. Trumper, "High-precision magnetic levitation stage for photolithography," *Precision Engineering-journal of The International Societies for Precision Engineering and Nanotechnology*, vol. 22, pp. 66–77, 1998.

[25] D. K. Bwambok, M. M. Thuo, M. B. Atkinson, K. A. Mirica, N. D. Shapiro, and G. M. Whitesides, "Paramagnetic ionic liquids for measurements of density using magnetic levitation," *Analytical chemistry*, vol. 85, no. 17, pp. 8442–8447, 2013.

[26] K. Mirica, S. Phillips, S. Shevkoplyas, and G. Whitesides, "Using magnetic levitation to distinguish atomic-level differences in chemical composition of polymers, and to monitor chemical reactions on solid supports," *Journal of the American Chemical Society*, vol. 130, pp. 17678–80, 2008.

[27] K. A. Mirica, S. S. Shevkoplyas, S. T. Phillips, M. Gupta, and G. M. Whitesides, "Measuring densities of solids and liquids using magnetic levitation: fundamentals," *Journal of the American Chemical Society*, vol. 131, no. 29, pp. 10049–10058, 2009.

[28] A. Winkleman, R. Perez-Castillejos, K. Gudiksen, S. Phillips, M. Prentiss, and G. Whitesides, "Density-based diamagnetic separation: Devices for detecting binding events and for collecting unlabeled diamagnetic particles in paramagnetic solutions," *Analytical chemistry*, vol. 79, no. 17, pp. 6542–50, 2007.

[29] I. Lyuksyutov, A. Lyuksyutova, D. Naugle, and K. Rathnayaka, "Trapping microparticles with strongly inhomogeneous magnetic fields," *Modern Physics Letters B*, vol. 17, no. 17, pp. 935–940, 2003.

[30] E. Feinstein and M. Prentiss, "Three-dimensional self-assembly of structures using the pressure due to a ferrofluid in a magnetic field gradient," *Journal of Applied Physics*, vol. 99, no. 6, p. 064901, 2006.

[31] H. Chetouani, C. Jeandey, V. Haguet, H. Rostaing, C. Dieppedale, and G. Reyne, "Diamagnetic levitation with permanent magnets for contactless guiding and trapping of microdroplets and particles in air and liquids," *Magnetics, IEEE Transactions on*, vol. 42, no. 10, pp. 3557 – 3559, 2006.

[32] S. Ge, A. Nemiroski, K. A. Mirica, C. R. Mace, J. W. Hennek, A. A. Kumar, and G. M. Whitesides, "Magnetic levitation in chemistry, materials science, and biochemistry," *Angewandte Chemie International Edition*, vol. 59, no. 41, pp. 17810–17855, 2020.

[33] E. Turker and A. Arslan-Yildiz, "Recent advances in magnetic levitation: a biological approach from diagnostics to tissue engineering," *ACS Biomaterials Science & Engineering*, vol. 4, no. 3, pp. 787–799, 2018.

[34] N. Shapiro, S. Soh, K. Mirica, and G. Whitesides, "Magnetic levitation as a platform for competitive protein-ligand binding assays," *Analytical chemistry*, vol. 84, pp. 6166–72, 2012.

[35] N. D. Shapiro, K. A. Mirica, S. Soh, S. T. Phillips, O. Taran, C. R. Mace, S. S. Shevkoplyas, and G. M. Whitesides, "Measuring binding of protein to gel-bound ligands using magnetic levitation," *Journal of the American Chemical Society*, vol. 134, no. 12, pp. 5637–5646, 2012.

[36] E. E. L. Lewis, H. Wheadon, N. Lewis, J. Yang, M. Mullin, A. Hursthouse, D. Stirling, M. J. Dalby, and C. C. Berry, "A quiescent, regeneration-responsive tissue engineered mesenchymal stem cell bone marrow niche model via magnetic levitation," *ACS nano*, vol. 10, no. 9, pp. 8346–8354, 2016.

[37] G. R. Souza, J. R. Molina, R. M. Raphael, M. G. Ozawa, D. J. Stark, C. S. Levin, L. F. Bronk, J. S. Ananta, J. Mandelin, M.-M. Georgescu, *et al.*, "Three-dimensional tissue culture based on magnetic cell levitation," *Nature nanotechnology*, vol. 5, no. 4, pp. 291–296, 2010.

[38] W. L. Haisler, D. M. Timm, J. A. Gage, H. Tseng, T. Killian, and G. R. Souza, "Three-dimensional cell culturing by magnetic levitation," *Nature protocols*, vol. 8, no. 10, pp. 1940–1949, 2013.

[39] H. Tekin, N. Durmus, S. Guven, K. Sridhar, A. Arslan Yildiz, G. CALIBASI KOCAL, I. Ghiran, R. Davis, L. Steinmetz, and U. Demirci, "Magnetic levitation of single cells," *Proceedings of the National Academy of Sciences*, vol. 112, pp. E3661—E3668, 2015.

[40] A. Turnbull and H. Hull, "A thermodynamic study of the dimerization of cyclopentadiene," *Australian Journal of Chemistry*, vol. 21, no. 7, pp. 1789–1797, 1968.

[41] M. Anil-Inevi, S. Yaman, A. Arslan Yildiz, G. Mese, O. yalcin ozuysal, H. Tekin, and E. Ozcivici, "Biofabrication of in situ self assembled 3d cell cultures in a weightlessness environment generated using magnetic levitation," *Scientific Reports*, vol. 8, p. 7239, 2018.

[42] K. A. Mirica, F. Ilievski, A. K. Ellerbee, S. S. Shevkoplyas, and G. M. Whitesides, "Using magnetic levitation for three dimensional self-assembly," *Advanced Materials*, vol. 23, no. 36, pp. 4134–4140, 2011.

[43] M. Atkinson, D. Bwambok, J. Chen, P. Chopade, M. Mwangi Thuo, C. Mace, K. Mirica, A. Kumar, A. Myerson, and G. Whitesides, "Using magnetic levitation to separate mixtures of crystal polymorphs," *Angewandte Chemie (International ed. in English)*, vol. 52, no. 39, pp. 1–5, 2013.

[44] N. Xia, P. Zhao, J. Xie, C. Zhang, J. Fu, and L.-S. Turng, "Defect diagnosis for polymeric samples via magnetic levitation," *NDT & E International*, vol. 100, pp. 175–182, 2018.

[45] B. Mann and N. Sims, "Energy harvesting from the nonlinear oscillations of magnetic levitation," *Journal of sound and vibration*, vol. 319, no. 1-2, pp. 515–530, 2009.

[46] G. Aldawood, H. T. Nguyen, and H. Bardaweel, "High power density spring-assisted nonlinear electromagnetic vibration energy harvester for low base-accelerations," *Applied Energy*, vol. 253, p. 113546, 2019.

[47] P. Carneiro, M. P. S. dos Santos, A. Rodrigues, J. A. Ferreira, J. A. Simões, A. T. Marques, and A. L. Kholkin, "Electromagnetic energy harvesting using magnetic levitation architectures: A review," *Applied Energy*, vol. 260, p. 114191, 2020.

[48] M. P. Soares dos Santos, J. A. Ferreira, J. A. Simões, R. Pascoal, J. Torrão, X. Xue, and E. P. Furlani, "Magnetic levitation-based electromagnetic energy harvesting: a semi-analytical non-linear model for energy transduction," *Scientific reports*, vol. 6, p. 18579, 2016.

[49] Y. Zhu, J. W. Zu, and L. Guo, "A magnetoelectric generator for energy harvesting from the vibration of magnetic levitation," *IEEE Transactions on Magnetics*, vol. 48, no. 11, pp. 3344–3347, 2012.

[50] J. Kaloust, C. Ham, J. Siehling, E. Jongekryg, and Q. Han, "Nonlinear robust control design for levitation and propulsion of a maglev system," *IEE Proceedings-Control Theory and Applications*, vol. 151, no. 4, pp. 460–464, 2004.

[51] C.-M. Huang, J.-Y. Yen, and M.-S. Chen, "Adaptive nonlinear control of repulsive maglev suspension systems," *Control Engineering Practice*, vol. 8, no. 12, pp. 1357–1367, 2000.

[52] J. Jansen, J. Smeets, T. Overboom, J. Rovers, and E. Lomonova, "Overview of analytical models for the design of linear and planar motors," *IEEE Transactions on Magnetics*, vol. 50, no. 11, p. 8206207, 2014.

[53] C. Truesdell and W. Noll, "The non-linear field theories of mechanics," in *The non-linear field theories of mechanics*, pp. 1–579, Springer, 1992.

[54] Z.-J. Yang and M. Tateishi, "Adaptive robust nonlinear control of a magnetic levitation system," *Automatica*, vol. 37, no. 7, pp. 1125–1131, 2001.

[55] A. El Hajjaji and M. Ouladsine, "Modeling and nonlinear control of magnetic levitation systems," *IEEE Transactions on industrial Electronics*, vol. 48, no. 4, pp. 831–838, 2001.

[56] M. M. * and R. Becerril, "Modelling and control design for a magnetic levitation system," *International Journal of Control*, vol. 77, no. 10, pp. 964–977, 2004.

[57] J. Jansen, C. Van Lierop, E. A. Lomonova, and A. Vandenput, "Modeling of magnetically levitated planar actuators with moving magnets," *IEEE Transactions on Magnetics*, vol. 43, no. 1, pp. 15–25, 2007.

[58] F.-J. Lin, L.-T. Teng, and P.-H. Shieh, "Intelligent adaptive backstepping control system for magnetic levitation apparatus," *IEEE transactions on magnetics*, vol. 43, no. 5, pp. 2009–2018, 2007.

[59] Y.-C. Lai, Y.-L. Lee, and J.-Y. Yen, "Design and servo control of a single-deck planar maglev stage," *IEEE Transactions on Magnetics*, vol. 43, no. 6, pp. 2600–2602, 2007.

[60] R.-J. Wai, J.-D. Lee, and K.-L. Chuang, "Real-time pid control strategy for maglev transportation system via particle swarm optimization," *IEEE Transactions on Industrial Electronics*, vol. 58, no. 2, pp. 629–646, 2010.
[61] F. Impinna, J. G. Detoni, N. Amati, and A. Tonoli, "Passive magnetic levitation of rotors on axial electrodynamic bearings," *IEEE Transactions on Magnetics*, vol. 49, no. 1, pp. 599–608, 2013.
[62] S. Folea, C. I. Muresan, R. De Keyser, and C. M. Ionescu, "Theoretical analysis and experimental validation of a simplified fractional order controller for a magnetic levitation system," *IEEE transactions on control systems technology*, vol. 24, no. 2, pp. 756–763, 2016.
[63] M. H. Yaseen and H. J. Abd, "Modeling and control for a magnetic levitation system based on simlab platform in real time," *Results in Physics*, vol. 8, pp. 153–159, 2018.
[64] R.-J. Wai and J.-D. Lee, "Robust levitation control for linear maglev rail system using fuzzy neural network," *IEEE transactions on control systems technology*, vol. 17, no. 1, pp. 4–14, 2009.
[65] R. Morales, V. Feliu, and H. Sira-Ramirez, "Nonlinear control for magnetic levitation systems based on fast online algebraic identification of the input gain," *IEEE Transactions on control systems technology*, vol. 19, no. 4, pp. 757–771, 2011.
[66] H.-J. Shieh, J.-H. Siao, and Y.-C. Liu, "A robust optimal sliding-mode control approach for magnetic levitation systems," *Asian Journal of Control*, vol. 12, no. 4, pp. 480–487, 2010.
[67] R. Fittro and C. Knospe, "Rotor compliance minimization via $\mu$-control of active magnetic bearings," *IEEE Transactions on Control Systems Technology*, vol. 10, no. 2, pp. 238 – 249, 2002.
[68] K. Prytz, *Electrodynamics: The Field-Free Approach*. 03 2015.
[69] R. Feynman, R. Leighton, and M. Sands, *The Feynman lectures on physics: mainly electromagnetism and matter*. 6th ed. Massachusetts: Addison-Wesley, 1977.
[70] M. NAYFEH and M. BRUSSEL, *Electricity and Magnetism*. I. ed. Singapore: John Wiley, 1985.
[71] Humusoft, "CE 152 Magnetic levitation model - Educational manual," 1996.
[72] Humusoft, "MF 634," 2022.